Intrinsic slip on hydrophobic surfaces

M. Chinappi[1], C.M. Casciola[1]
[1] *Dipartimento Meccanica e Aeronautica, Università di Roma "La Sapienza", via Eudossiana 18, 00184, Roma, Italia*
E-mail: mauro.chinappi@uniroma1.it, carlomassimo.casciola@uniroma1.it

Keywords:
nanofluidics, slip length, molecular dynamics, self assembled monolayers

SUMMARY.
Continuum models often fail to correctly describe fluids in micro and nano devices. For simple fluids departures from the standard behavior could be ascribed to inappropriateness of the continuum assumption and to violations of the no-slip condition. In fact liquids behave as continua, with the exception of extreme confinement on length scales of few molecular diameters, where a new regime – single file motion – sets in [1]. Instead, slippage at the wall is frequently observed, the flow field considerably differing from classical predictions. In the present paper the intrinsic slip is addressed via Molecular Dynamics simulations of a Couette flow of liquid water on a hydrophobic surface formed by a Lennard-Jones solid coated with a Self Assembled Monolayer (SAM) of octadecyltrichlorosilane (OTS), a widely used technology for wall functionalization. The model reproduces several features of the OTS-SAM coating, e.g. contact angle of water and the tilting of OTS molecules with respect to the surface normal. The system exhibits slippage and the orientation of the OTS molecules is found to induce a preferential slip direction. Overall, the inferred slippage cannot explain the larger slip length measured in experiments, providing indirect evidence of apparent slip, presumably due to gas trapping at the surface.

1 Introduction

Several recent experimental studies [13, 16, 11, 2, 4] definitively proved that the no-slip boundary condition is inappropriate to describe the fluid/solid interface for several microfluidic systems. A more general description is given by the Navier boundary condition

$$\mathbf{u}_w = L_s \mathbf{n} \cdot [\nabla \mathbf{u} + (\nabla \mathbf{u})^T] \cdot (\mathbf{I} - \mathbf{n} \otimes \mathbf{n}), \tag{1}$$

where $\mathbf{u}_w$ is the velocity at the wall, $\mathbf{n}$ the wall normal and L_s a parameter called slip length. The usual case of no slip condition is recovered for $L_s = 0$, while $L_s \to \infty$ corresponds to free slip interfaces. The basic conceptual experiment concerning the slip length consists of a micro channel with an enforced pressure difference between entrance and exit sections. By comparing the measured flow rate through the microchannel with the expression provided by the Stokes equations with the Navier boundary condition, an effective slip length can be inferred. The values of L_s found in the literature [13], ranging from zero to few microns, show the strong dependence on different features of the solid-liquid interfaces – such as chemical composition, roughness and dissolved gases.

Two different mechanisms have been propose to explain slippage. i) The first mechanism addresses the intermolecular interaction between liquid and wall atoms, which drastically affects the structure of the first layers of liquid molecules close to the interfaces. Strong attractive interactions (hydrophilic surface) induce an ordered layering of liquid atoms leading to a sort of freezing of the first layer. In this case the observed slip length is slightly negative. On the other hand a weak interaction (hydrophobic surface) allows the slippage of liquid molecules on the solid leading to positive

L_s. This scenario is often referred to as intrinsic slip [10]. ii) The second mechanisms involves a gaseous phase trapped at the wall, in the form of either a gas layer or gas nanobubbles. In this case the observed slip of the liquid is ascribed to a sort of free slip boundary condition at the liquid-gas interface. We will refer to this scenario as apparent slip [10]. For both mechanisms the chemical composition of the surface plays a crucial role. Actually for intrinsic slip chemical interactions directly influence the slippage while, for apparent slip, the chemical composition enters though the wettability of the surface and, hence, though the capability of the wall to trap the gaseous phase.

A common procedure to alter the solid surface properties to control slippage is coating the wall with a Self Assembled Monolayer (SAM). SAMs are layers of amphiphilic molecules in which one end (interior end) of the molecule shows affinity for the solid substrate and the other end (exposed end) can be functionalized to obtain desired properties, e.g. hydrophobicity. Several authors [2, 4, 16, 3] analyzed the effect of SAM formed by Octadecyltriclorosilane (OTS) on the slippage of liquid water reporting slip length ranging between $20nm$ and $1\mu m$. The issue is still debated since available experimental procedures do not clearly discriminate between intrinsic and apparent slip mechanisms.

In this study we use non equilibrium molecular dynamics simulation (NEMD) to estimate the intrinsic slip length L_s for water-OTS interface using a Couette flow geometry. Preliminarily, the wettability of the interface is characterized by measuring the contact angle in equilibrium conditions. In comparison with available experimental data, our results strongly suggest that intrinsic slip cannot explain the large slip-length found in the experiments leaving issues for further explorations even in cases where experiments did not provide direct evidence of trapped gas at the wall.

2 Simulation setup

2.1 Water drop on OTS-SAM surface

OTS-SAMs are known to assemble in hexagonal cells with a typical surface density of around $1/22$ molecules for $\mathring{A}^2$ [8]. To build a reasonable model of the system, a suitable substrate sharing the same geometric characteristics is instrumental. Our substrate solid wall is constituted by a face centered cubic (fcc) crystal of Lennard-Jones atoms of mass m_w whose 111 planes have the same hexagonal structure of OTS-SAMs. The Lennard-Jones parameters σ_w and ϵ_w are chosen to achieve an atom density on 111 planes $\rho_{111} = 1./22.\mathring{A}^{-2}$ at a temperature of $300K$ and a pressure of $1atm$, hence matching the SAM surface density. Clearly at the simulation temperature ($300K$) the virtual solid must be far from the melting point. An iterative procedure based on a set of thermostated and barostated simulations (NPT) at $300K$ and $1atm$ led to select the following parameters: $m_w = 70\ amu$, $\epsilon_w/k_b = 1258K$, with k_b the Boltzmann constant, and $\sigma_w = 4.555\mathring{A}$. The corresponding fcc cell dimension is $a = 7.13\mathring{A}$ while the distance among contiguous atoms in 111 planes is $d = 5.04\mathring{A}$.

The Octadecyltrichlorosilane $CH_3(CH_2)_{17}SiCl_3$ (OTS) is formed by a linear alkyl of 17 carbon atoms with a methyl group on one end and a $SiCl_3$ group on the other one. During the formation of the monolayer, the chloride atoms are substituted with OH groups. In the final configuration, the interior end – $Si(OH)_3$ – of contiguous OTS molecules are covalently bound together via Si-O-Si bridges formed by expelling a water molecule. The bridges provide stability to the monolayer. We assume that the detailed chemistry leading to the adhesion of the monolayer to the substrate (inner side of SAM) is largely irrelevant to its interaction with the liquid water (outer side). Hence we drastically simplify the model by substituting the interior end with a Lennard-Jones (LJ) atom of the same type used for the wall. The behavior of these LJ atoms in the simulation needs a brief description.

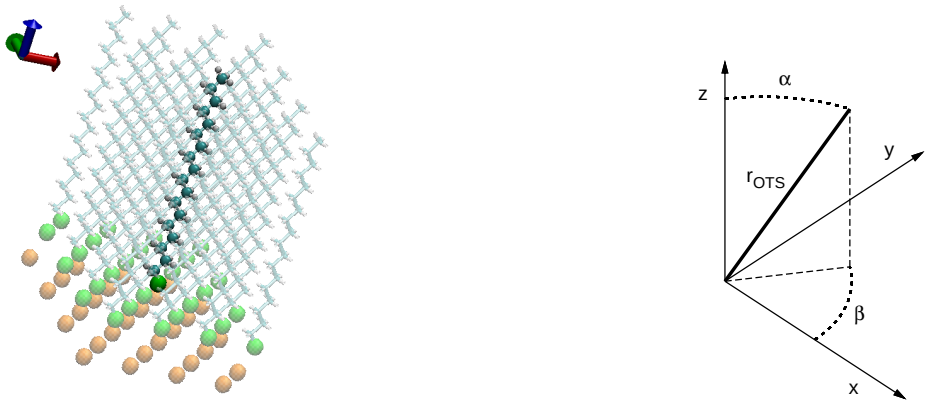

Figure 1: Left panel. The OTS molecule (azure) is modelled as a 17 carbon atoms alkyl chain completed with the exposed methyl group and the hybrid LJ atom (green) forming the interior end. LJ hybrid atoms are arranged as a 111 plane of the face centered cubic structure. In orange, the 111 plane of the solid crystal, parallel to Oxy. In the initial configuration, the OTS molecules are normal to wall plane. Image created with VMD [6]. Right panel. Sketch of OTS orientation and nomenclature. The tilting angle α is the angle between z-axis and the molecule axis, $\mathbf{r}_{OTS}$, oriented from the interior end of the OTS (hybrid LJ atom) to the Carbon atom of the exposed end. The azimuth β is the angle between the x axis and the projection of the molecule on Oxy plane.

Overall we use the charmm27 force field [12]. In this context two kinds of interactions occur among different atoms, non-bonded and bonded, respectively. Bonded interactions take place among atoms of the same molecule whenever their distance in the topological structure is less than four covalent bonds. Non bonded interactions (Lennard-Jones and Couloumbian forces) occur among atoms with larger distances in the same molecule or among atoms belonging to different molecules. The LJ atom used as interior group of OTS molecules behaves in a hybrid way: as a carbon atom of a methyl group of the alkyl chain as concerning bonded interactions and as a standard wall atom as concerning non-bonded ones. Water is treated with the TIP3P model, as often in the charmm27 context. A cutoff radius of $12\mathring{A}$ was used for Van Der Vaals interactions.

Figure 1 shows a sketch of the molecular arrangement used for the initial configuration of crystal and OTS. The azure chains represent the OTSs, whose interior end made of the hybrid atom is displayed in green. The orange beads represent the 111 plane of the standard LJ atoms of the crystal. The hybrid LJ atoms forming the interior end of the OTS molecules are arranged as if they were a further atomic layer at the surface of the crystal. The figure highlights a single OTS molecule in a bunch of neighbors in its initial configuration normal to the 111 plane of the crystal taken as the Oxy coordinate plane. The overall system consists of four 111 layers formed by 625 LJ atoms each, on top of which we arrange the OTS monolayer consisting of 625 molecules. The atoms belonging to the lower 111 plane of the solid are keep fixed during the MD simulation. A pre-equilibrated TIP3P water drop was added to the system using the VMD solvate package [6]. Periodic boundary conditions are applied in all directions, being $L_x = 126\mathring{A}$, $L_y = 109.11\mathring{A}$ and $L_z = 128\mathring{A}$ the box dimensions. For comparison, a setup of a LJ wall with no OTS-SAM was prepared using the same

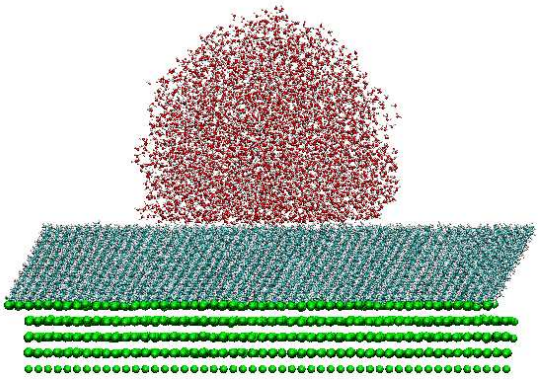

Figure 2: Snapshot of a simulation: a water drop (red) lies on a OTS-SAM (azure) coating the 111 surface of a Lennard-Jones solid (green). The snapshot was taken after the equilibration condition is reached. A contact angle larger than $\pi/2$ is apparent. The system is formed by 625 OTS molecules, 2500 Lennard-Jones atoms and 4802 water molecules. The wall is parallel to Oxy plane, the box dimensions are $L_x = 126\mathring{A}$, $L_x = 109.11\mathring{A}$ and $L_x = 128\mathring{A}$. Image created with VMD [6]

.

procedure (Fig. 3).

2.2 Couette flow on the OTS-SAM surface

The three ingredients (LJ solid, OTS-SAM and water) of the equilibrium simulation of a water drop on a coated LJ wall are also used for simulating the Couette flow between two parallel walls. The equilibration procedure to be described below is performed using a Langevin piston [15] to control density, implying that the volume available to liquid water changes along the equilibration process. Each wall is formed by five 111 planes of LJ solid, 324 atoms each. The lower wall is coated with a SAM formed by 324 OTS molecules (Fig. 4). The initial configuration is created adding water molecules (VMD solvate package [6]) between the two solid walls. The initial distance between the lower plane of the coated wall and the upper plane of non-coated wall is $157.89\mathring{A}$. As in the case

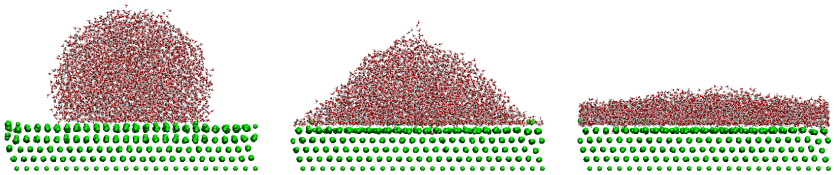

Figure 3: Snapshots of water (red) spreading on 111 Lennard-Jones solid surface (green). Left, $t = 0$. Center, $t = 0.6\ ns$. Right, $t = 2.4\ ns$. The system is formed 3125 Lennard-Jones atoms and 4802 water molecules. As in Fig 2, the wall is parallel to the Oxy plane and the box dimensions are $L_x = 126\mathring{A}$, $L_x = 109.11\mathring{A}$ and $L_x = 128\mathring{A}$. Image created with VMD [6]

.

simulation	forcing (pN)	Plate vel $(\mathring{A}/ps)$	slip length $(\mathring{A})$
A	0	0	not defined
B	$100.24\,\hat{\mathbf{y}}$	0.0195	4.5
C	$-100.24\,\hat{\mathbf{y}}$	-0.0201	8.5
D	$100.24\,\hat{\mathbf{x}}$	0.0225	6.3
E	$-100.24\,\hat{\mathbf{x}}$	-0.0194	5.8

Table 1: List of the simulations. The total force applied to the upper plate made of 1620 Lennard-Jones atoms is provided under the heading "forcing". The force is equally distributed on each atom of the plate and the corresponding average stress exerted by the plate on the fluid is $1.4067 * 10^6 Pa$. Case A is the equilibrium simulation used to estimate the density profile reported in right panel of Fig. 5.

of the drop, the OTS molecules were initially placed normal to the surface. A triperiodic NPT simulation with a Langevin piston (piston period $100ps$, piston decay $50ps$ [15]) was performed in order to reach the target thermodynamic state. The initial box dimensions are $L_x = 90.72\mathring{A}$, $L_y = 78.57\mathring{A}$ and $L_z = 162\mathring{A}$. In the initial configuration, the top wall (non-coated) of the basic computational domain and the bottom wall (coated) of its periodic image above form a unique brick of ten 111 planes of LJ atoms. During the NPT simulation L_x, L_y and L_z were allowed to vary independently, in response to the corresponding normal component of the pressure tensor. The left panel of Fig. 5 shows the time evolution of the three box dimensions normalized by the initial value. After a sharp change in the first few time steps (the detail is too small to be appreciated in the drawing) smooth convergence to the equilibrium value is observed. While L_x and L_y essentially keep their initial values, L_z decreases significantly. The five percent deviation in L_z is partially explained by the tilting of the OTS molecules and partially by the amount of bulk water inserted in the initial state, smaller than required to exactly fill the available volume.

After equilibration the two walls originally forming a unique brick, are separated adding a void of suitable thickness. Purpose of the added void region is isolating the base computational cell from the interactions with its periodic images in the wall-normal direction. The thickness of the void was found to be irrelevant as soon as it exceeds the cutoff radius of Van Der Vaals interactions. In our simulations the thickness is $15\mathring{A}$, 1.25 times the cutoff radius. To keep a fixed distance between the walls, atoms belonging to the lower plane of the coated wall are fixed, while those of the upper plane of the uncoated wall are restrained vertically by a harmonic potential $U_c = 1/2k(z_i - z_{i0})^2$ with $k = 10.Kcal/(mol\,\mathring{A})$ and z_{i0} the position at the end of equilibration phase. This configuration was used as initial condition for several equilibrium and non equilibrium simulations. The Couette simulation is realized by setting the uncoated wall into motion by a constant force along the Oxy plane acting on each LJ atom. The moving wall drags along the liquid until a steady shear flow develops. The energy injected by the external forcing is removed by a Langevin thermostat (time constant $5ps$) acting on the LJ atoms of the coated wall. All the simulations have been performed with the NAMD software [15].

3 Results

3.1 Contact angle

As described in section 2.1 the initial configuration is formed by an OTS layer in which every molecule is normal to the wall. A TIP3P water drop of radius $r = 35\mathring{A}$, centered $20\mathring{A}$ above the plane of Carbon atoms belonging to the exposed end of OTS molecules, was placed on the coated

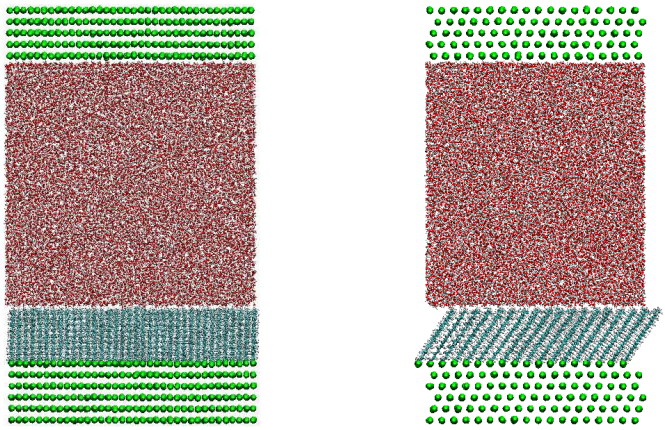

Figure 4: Snapshot of the Couette flow geometry with the OTS-SAM coating after equilibration. Water (red) is confined between the two plane walls (green) formed by five 111 planes of 324 LJ atoms each, the lower wall being coated with 324 OTS molecules (azure). A total amount of 85134 atoms is used, with box dimensions of $90.3\mathring{A} \times 79.2\mathring{A} \times 153.9\mathring{A}$. In the Couette flow simulations, after introducing a suitable void to isolate the basic computational cell from its neighbors in the wall normal direction, a constant force is applied to the upper plate to drive the wall. The lower wall is kept at rest. Left panel, Ozy view. Right panel, Ozx view.

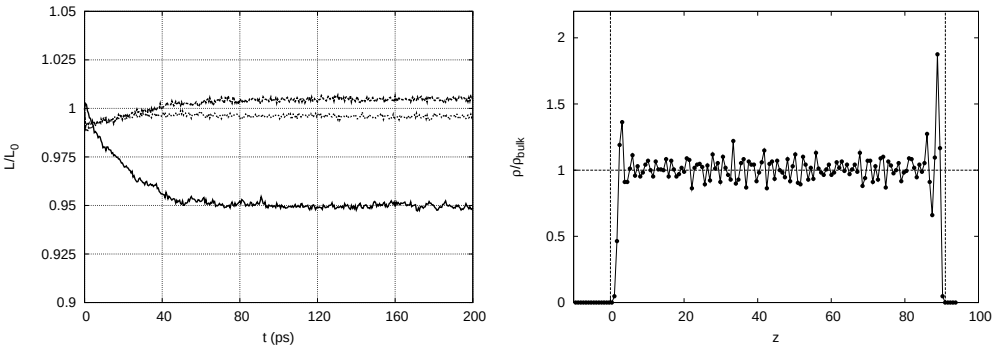

Figure 5: Left panel. Time evolution of the box dimensions normalized by their initial values. After a sharp change in the first few time steps (though hardly seen in the plot, the curves actually start at $1.d0$), relatively smooth convergence to the equilibrium values is achieved. L_x and L_y substantially keep their initial values. L_z instead decreases significantly. Right panel. Density profile in the nanochannel normalized with the bulk value ρ_{bulk}. The nominal positions of the wall surfaces are shown by the two vertical lines. They are defined as average of the z-coordinates of Carbon atoms belonging to OTS exposed ends as concerning the coated wall, and as average of the z-coordinate of the Lennard-Jones solid 111 plane atoms closest to the water for the opposite uncoated surface. The OTS nominal interface is at $z = 0$. Apparently, the water molecules distribution is different at the two walls, showing a larger peak at the Lennard-Jones, hydrofilic wall.

wall. A $1200ps$ NVT simulation (Langevin thermostat time constant $5ps$) was performed to relax the system to equilibrium. During the equilibration the OTS molecules spontaneously tilted (Fig. 2). Two parameters are introduced to characterize the OTS tilting, namely the tilting angle α and the azimuthal angle β measured from the positive x-axis. The right panel of Fig. 1 shows the axis of the OTS molecule, $\mathbf{r}_{OTS} = \mathbf{r}_{LJ} - \mathbf{r}_{C18}$, where $\mathbf{r}_{LJ}$ is the position of the hybrid LJ atom of the interior end and $\mathbf{r}_{C18}$ that of the Carbon atom of the exposed end. Denoting the unit vector along the molecule axis by $\hat{\mathbf{r}}_{OTS}$, the average tilting angle is defined as $\langle\alpha\rangle = \langle\cos^{-1}(\hat{\mathbf{z}} \cdot \hat{\mathbf{r}}_{OTS})\rangle$ where $\hat{\mathbf{z}}$ is the unit vector along the z-axis and the average implied by the angular brackets is performed on all the OTS molecules over several equilibrium configurations. The azimuth is the angle β between the unit vector $\hat{\mathbf{x}}$ along the x-axis and the direction of the molecule projection on the wall plane $0xy$, i.e. $\beta = \cos^{-1}\left[\hat{\mathbf{x}} \cdot (\hat{\mathbf{r}}_{OTS} - \hat{\mathbf{r}}_{OTS} \cdot \hat{\mathbf{z}}) / |\hat{\mathbf{r}}_{OTS} - \hat{\mathbf{r}}_{OTS} \cdot \hat{\mathbf{z}}|\right]$. The tilting angle is a rather robust feature. For the simulation addressed here we observe very small fluctuations (standard deviation $\Delta_\alpha = 2.2°$) around the mean value $\langle\alpha\rangle = 32.5°$ in agreement with literature results [7]. As we will see, this typical value is reproduced also in the Couette simulations to be discussed in the next session. Concerning the azimuth, its average value is rather sensitive to the specific initial conditions, as expected on the basis of symmetry considerations. Nonetheless, for a specific case also this observable is found to present very small fluctuations (standard deviation $\Delta_\beta = 3.6°$), implying an ordered structure of the monolayer.

After equilibration, the thermostat is switched off to run a $1200ps$ long nanochannel (NVE) simulation with the purpose of estimating the contact angle θ of the drop. An overall impression on the drop geometry is gained by looking at figure 2, showing clearly the hydrophobicity of the surface. However inferring a quantitative measure requires some care. To measure the contact angle the following procedure has been devised. i) First the nominal wall surface was defined as the Oxy-plane characterized by the equation $z = \langle z_{C18}\rangle$, where $C18$ denotes the Carbon atom belonging to the OTS molecules exposed end. ii) Positions of water molecules are tagged by the respective Oxygen atoms, whose spatial distribution is estimated by binning on a cubic grid with size $\Delta = 2.\mathring{A}$. iii) Moving from the bulk of the drop towards the exterior the water molecules density drops abruptly across the interface. The surface of the drop is defined by the positions of the grid cell centers where the Oxygen atoms density lies in the range $0.45 - 0.55\rho_{bulk}$, with ρ_{bulk} the bulk density. To avoid contamination from layering effects close to the wall, only grid points farther than $5\mathring{A}$ from the nominal wall surface are accounted for. iv) After fitting these surface points by a sphere, the contact angle θ is defined as the angle between sphere and nominal wall plane.

The reported procedure provided the estimate $\theta \simeq 128°$. The algorithm is rather stable with respect to variations of the parameters. A more significant difference ($\theta = 123°$) in angle is obtained instead by shifting the nominal wall surface towards the liquid by one Van der Waals radius, [5]. We stress that the contact angle is independent from the specific initial conditions, as was checked by repeating the simulation with different initial drop positions. Irrespective of the specific definition, the present result is slightly larger than found in experiments, where the measured contact angle ranges from $100°$ to $120°$ [16, 9, 3, 14]. Fig. 3 shows successive snapshots in absence of the OTS coating, providing evidence of the complete wettability of the uncoated surface.

3.2 Equilibrium properties of the coated nanochannel

Before discussing the effect of OTS-SAMs on slippage, we analyze the equilibrium properties (no flow) of the nano-channel filled with water molecules, figure 4. During the equilibration phase, described in section 2.2, the SAM molecules are observed to spontaneously tilt. The average tilting angle $\langle\alpha\rangle$ is the same found in the drop simulation, confirming the robustness of this observable.

Concerning the azimuth β, in principle any value is equally likely given the symmetry of the configuration. For the equilibrium configuration used as common initial condition for all the Couette flow simulations to be described below the azimuth happened to be $\beta = -90.1°$, corresponding to projections of the OTS molecules in the negative $\hat{\mathbf{y}}$ direction. The Oxygen equilibrium density distribution as a function of wall normal coordinate z was obtained from a $1200ps$ NVE simulation. The right panel of Fig. 5 reports the density profile estimated by binning the channel into $0.7\mathring{A}$-thick wall-parallel slabs, normalized with the bulk value ρ_{bulk}. The usual layering of liquids is comparatively much more apparent at the Lennard-Jones wall than at the OTS coated surface, in line with the result of the drop simulation where the OTS-SAM showed hydrophobic behavior in contrast to the hydrophilic Lennard-Jones solid.

3.3 Slippage on OTS-SAM coating

The response of the system to different shear conditions is analyzed in order to characterize the slip properties of the OTS-SAM coating. Unless extremely large shear rate are achieved, the slip-length is expected to be independent of shear rate, i.e. of force intensity. This properties has been preliminarily checked, showing that doubling the force the same slip length is reproduced within statistical accuracy. However, since our system presents a specific equilibrium orientation of the OTS molecules, it may suspected of anisotropy in the force-slip functional relationship. To check this feature the forcing has been applied in different directions as summarized in Table 2.2. Simulations B and C concern forcing along the positive and negative $\hat{\mathbf{y}}$ direction, respectively. Cases D and E concern the orthogonal direction. The strongest difference in response is found between cases B and C, when the forcing is aligned with the azimuth of the OTS molecules. The time history of the top wall center of mass velocity V (projected along the forcing direction) is reported in the left panels of Fig 6 for these two cases. Similar results (data not shown) are obtained for simulations D and E.

The systems takes about $0.6ns$ to reach the steady state after switching the forcing on. Fluctuations in the instantaneous center of mass velocity of the wall are expected and can be preliminarily estimated from energy equipartition. The thermal velocity of each wall particle is $v_\theta = (k_b\theta/m_w)^{1/2}$, implying that the corresponding center of mass velocity of the wall fluctuates with typical speed $V' = v_\theta/\sqrt{N} \simeq 0.04\mathring{A}/ps$, where N is the number of wall atoms, providing the order of magnitude of the noise observed in the left panel of Fig. 6.

The linear profile of the Couette flow is reproduced by the mean velocity, calculated in the steady state, sufficiently far from the wall. As expected, it slightly deviates very close to the wall (see right panels of Fig 6). The slip length L_s is estimated as the distance between nominal wall position and location where the velocity profile, fitted in the bulk region ($20\mathring{A} < z < 70\mathring{A}$), extrapolates to zero.

For case C (motion along the molecules azimuth) (left panel of Fig 6) the estimated slip length is $L_s = 8.5\mathring{A}$. As anticipated, this value is partially affected by the adopted definition of nominal wall surface. No universally accepted definition exists, see [5] for an alternative definition. In any case, depending on the choice, the slip length may hardly increase by more than $3 \div 4\mathring{A}$.

In case B (forcing in the reverse direction) the slip length is $4.5\mathring{A}$. The relative difference with the previous case is significant, indicating that the asymmetry of the OTS-SAM affects the slippage. The anisotropy is confirmed when forcing in the orthogonal directions (cases D and E, Table 2.2) where a common intermediate value for L_s is consistently found.

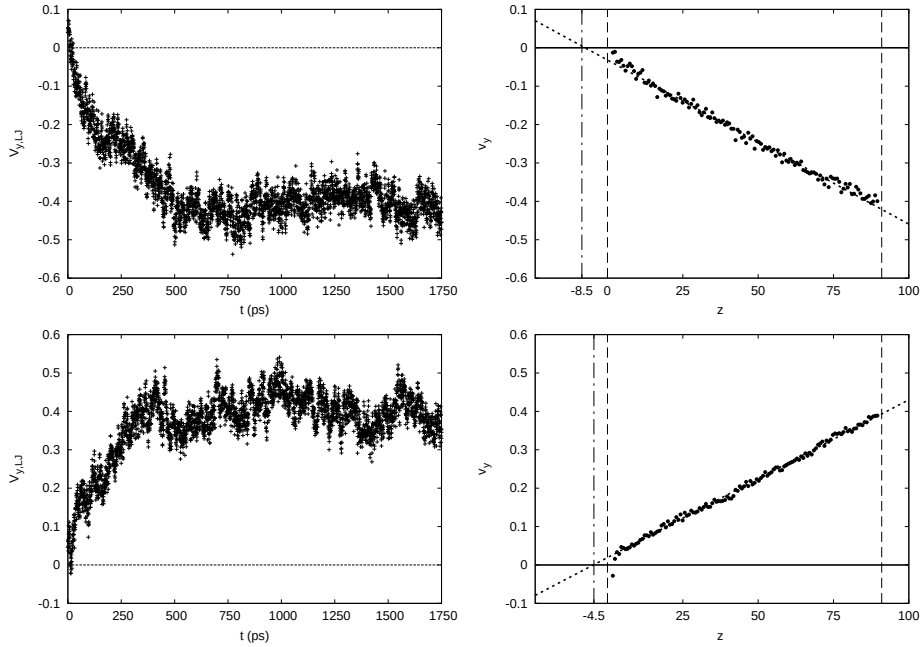

Figure 6: Upper Left. Center of mass velocity V (y component, in $\mathring{A}/ps$ units) of the upper solid plate for case C of table 2.2. Upper Right. Mean velocity profile ($\mathring{A}/ps$) for case C. The dotted line provides the fit in the bulk of the nanochannel. The vertical dashed lines at $z = 0\mathring{A}$ and $z = 91\mathring{A}$ denote the positions of the two walls. The fitted velocity profile differs from zero at the nominal interface and vanishes $8.5\mathring{A}$ inside the coated wall (dot-dashed line). Lower Left. Time evolution of V for case B. Lower Right. Mean profile for simulation B.

4 Concluding remarks

Slippage of liquid water at an OTS-SAM coated wall was analyzed with an all-atoms MD simulation. The purpose was understanding which mechanism, between intrinsic and apparent slip, better explains the published experimental results on the issue. Special care was devoted in checking the system response with respect to the main physical features of actual OTS coated interfaces. The OTS molecules were modeled to a certain level of detail, reasonably reproducing the equilibrium tilting angle of about $30\circ$, known from experiments. The wettability properties of the surface were extensively addressed, estimating the contact angle of water in $125 \pm 2\circ$, where the uncertainty is basically due the lack of a universally accepted definition of nominal wall surface. The contact angle slightly exceeds the values measured in experiments, overestimating somewhat the hydrophobicity of the water/OTS-SAM interface. Overall these results suggest the intrinsic slip as hardly responsible for the slippage of water at OTS-SAM surfaces, calling the attention to gas trapping at the wall, even in cases where no direct experimental evidence of the phenomenon exists.

A peculiar and unexpected feature of our system is the slippage anisotropy under different forcing directions, induced by the coherent tilting of the OTS molecules. Despite anisotropic slippage has been already reported in the context of patterned super-hydrophobic surfaces, to the best of our knowledge this is the first evidence of the effect at the molecular level.

5 Acknowledgement

Computing resources were made available by CASPUR under HPC Grant 2009.

References

[1] M. Chinappi, S. Melchionna, C.M. Casciola, and S. Succi. Mass flux through asymmetric nanopores: Microscopic versus hydrodynamic motion. *The Journal of Chemical Physics*, 129:124717, 2008.

[2] C.H. Choi, K.J.A. Westin, and K.S. Breuer. Apparent slip flows in hydrophilic and hydrophobic microchannels. *Physics of fluids*, 15:2897, 2003.

[3] C. Cottin-Bizonne, B. Cross, A. Steinberger, and E. Charlaix. Boundary slip on smooth hydrophobic surfaces: Intrinsic effects and possible artifacts. *Phys. Rev. Lett*, 94(056102):1–4, 2005.

[4] C. Cottin-Bizonne, S. Jurine, J. Baudry, J. Crassous, F. Restagno, and E. Charlaix. Nanorheology: An investigation of the boundary condition at hydrophobic and hydrophilic interfaces. *The European Physical Journal E-Soft Matter*, 9(1):47–53, 2002.

[5] D.M. Huang, C. Sendner, D. Horinek, R.R. Netz, and L. Bocquet. Water slippage versus contact angle: A quasiuniversal relationship. *Physical Review Letters*, 101:22, 2008.

[6] W. Humphrey, A. Dalke, and K. Schulten. VMD: Visual molecular dynamics. *Journal of Molecular Graphics*, 14(1):33–38, 1996.

[7] D.L. Irving and D.W. Brenner. Diffusion on a self-assembled monolayer: molecular modeling of a bound+ mobile lubricant. *J. Phys. Chem. B*, 110(31):15426–15431, 2006.

[8] K. Kojio, S. Ge, A. Takahara, and T. Kajiyama. Molecular aggregation state of n-octadecyltrichlorosilane monolayer prepared at an air/water interface. *Langmuir*, 14(5):971–974, 1998.

[9] A. Krishnan, Y.H. Liu, P. Cha, R. Woodward, D. Allara, and E.A. Vogler. An evaluation of methods for contact angle measurement. *Colloids and Surfaces B: Biointerfaces*, 43(2):95–98, 2005.

[10] E. Lauga, M.P. Brenner, and H.A. Stone. Microfluidics: The no-slip boundary condition. *Handbook of Experimental Fluid Dynamics, Chap 15*, 2005.

[11] C. Lee, CH Choi, and CJ Kim. Structured surfaces for a giant liquid slip. *Physical review letters*, 101(6):064501, 2008.

[12] AD MacKerell Jr, D. Bashford, M. Bellott, R.L. Dunbrack Jr, JD Evanseck, MJ Field, S. Fischer, J. Gao, H. Guo, S. Ha, et al. All-atom empirical potential for molecular modeling and dynamics studies of proteins. *J. Phys. Chem. B*, 102(18):3586–3616, 1998.

[13] C. Neto, D.R. Evans, E. Bonaccurso, H.J. Butt, and V.S.J. Craig. Boundary slip in Newtonian liquids: a review of experimental studies. *Reports on Progress in Physics*, 68(12):2859–2898, 2005.

[14] R.D. Peters, P.F. Nealey, J.N. Crain, and F.J. Himpsel. A near edge X-ray absorption fine structure spectroscopy investigation of the structure of self-assembled films of octadecyltrichlorosilane. *Langmuir*, 18(4):1250–1256, 2002.

[15] J.C. Phillips, R. Braun, W. Wang, J. Gumbart, E. Tajkhorshid, E. Villa, C. Chipot, R.D. Skeel, L. Kale, and K. Schulten. Scalable molecular dynamics with NAMD. *Journal of Computational Chemistry*, 26(16):1781, 2005.

[16] D.C. Tretheway and C.D. Meinhart. Apparent fluid slip at hydrophobic microchannel walls. *Physics of Fluids*, 14:L9, 2002.